

Influence of Aircraft Self-Shielding on World-Wide Calculations of Effective Dose Rates to Occupants

Kyle Copeland[1]
Numerical Sciences Research Team, Aerospace Medical Research Division, FAA, MMAC, CAMI, Oklahoma City, OK 73169 USA

and

William Atwell[2]
Retired Boeing Technical Fellow, Houston, TX 77058 USA

It is commonplace when calculating ionizing radiation exposures of aircraft occupants to neglect the influence of the aircraft's presence on the dose rate, which greatly simplifies calculations of dose rate. FAA technical report DOT/FAA/AM-17/8 describes a method of revising CARI-7 calculations to approximately account for aircraft structure when calculating effective dose rates based on the NASA Langley Research Center OLTARIS toolset, which yields results consistent with findings of earlier researchers, but without the need for detailed aircraft structure and loading models. The method is applied here to investigate the reasonableness of the common simplification on a global scale at typical flight levels from 30,000 to 60,000 feet, using effective vertical cutoff rigidity world-grids calculated by Smart and Shea. Shielded occupant dose rate is consistently reduced relative to the unshielded case, but the reduction in dose rate at cruise altitude is typically only a few percent at the levels of shielding considered (up to 1.27 cm Al-2024). Results thus indicate that the practice of ignoring this source of occupant shielding does not lead to large errors in effective dose rate calculations for flights in the altitude range examined. Effective doses for both solar minimum and solar maximum are discussed for a number of flight paths (routes) including several polar routes.

Nomenclature

E	=	effective dose
h_{atm}	=	atmospheric depth
h_{shield}	=	shield depth
K	=	dose correction factor

I. Introduction

Northern polar routes more closely follow a geodesic path and thus can be significantly faster and cheaper to operate than more traditional trans-Pacific routes. While once rare, they are now considered common (Cox, 2017).[1] However, these routes also come with increased difficulties in communications and environmental hazards, including potentially increased exposure of aircraft occupants and avionics to solar and galactic cosmic radiation. The common practice when calculating radiation exposures has been to neglect the shielding afforded occupants by the aircraft (Battistoni et al., 2005).[2] Numerous comparisons of measurement of doses on flights to code predictions, such as the EURADOS Report 2012-3, confirm this expectation to be true to within the accuracy of the codes and measurements (Bottollier-Depois, J. F. et al., 2012).[3] The vast bulk of the flight data and simulation work has been done at altitudes from of FL 400 and below.

As technology advances, there is an interest in higher altitudes for both manned and unmanned flight. U. S. Federal Aviation Administration technical report DOT/FAA/AM-17/8 describes a method of revising unshielded calculations to approximately account for aircraft presence when calculating effective dose rates at low cutoff

[1] Team Coordinator, Numerical Sciences Research Team, kyle.copeland@faa.gov.
[2] Retired Boeing Technical Fellow, william.atwell@boeing.com.

rigidities and high altitudes,[4] based on calculations using the National Aeronautics and Space Administration (NASA) Langley Research Center On-Line Tool for the Assessment of Radiation In Space (OLTARIS) toolset.[5] In this study, the method is adapted to examine shielded occupant effective dose rate relative to ignoring aircraft structure at altitude from FL 300 to FL 600, using common commercial aircraft structure (up to 1.27 cm of aerospace aluminum alloy Al-2024) as the added shielding. Effective doses for both solar minimum and solar maximum are discussed for a number of flight paths (routes), with the specific example of a U.S.-Asia polar route.

II. Methods

The FAA method replaces the shield material(s) with air, and then a material and depth dependent correction factor is applied using Eq (1).

$$E(h_{atm},h_{shield}) = E_{atm}(h_{atm} + h_{shield})K_{shield}(h_{atm},h_{shield}) \quad (1)$$

For this study, correction factors, *K*, were calculated from OLTARIS results relating effective dose equivalent inside air shells to mixed shield shells (50 g/cm^2 of ICRU dry air, with added Al-2024 alloy) of the same depth. Table 1 shows the correction factors for depths simulating a B-737 and a B-747, using shield thicknesses of 3/16" (0.476 cm) and 1/2" (1.27 cm) of Al-2024 alloy (density = 2.78 g/cm^3), respectively, calculated for the range of orbit averaged vertical cutoff rigidities that could be probed by OLTARIS (0-14 GV).

Table 1. Shielding correction factors for B-737 and B-747 Al-2024 alloy.

Orbit Average Vertical Cutoff Rigidity (GV)	Effectiveness Factor, K			
	B-737 at Solar Max.	B-737 at Solar Min.	B-747 at Solar Max.	B-747 at Solar Min.
0	1.003	1.002	1.007	1.006
7	1.004	1.002	1.008	1.007
14	1.004	1.003	1.008	1.008

In addition to using Al-2024 alloy instead of pure aluminum, orbit average dose rates were used instead of orbits at 1 AU. This change from the method of the FAA report was needed to allow calculations at non-zero cutoff rigidities. When compared with the coefficients calculated for pure aluminum at 0 GV and solar minimum conditions in the FAA report (1.002 and 1.003, respectively) the coefficients for the alloy were slightly larger (1.002, 1.006). Some changes in *K* values relative to the FAA report were expected because of added high mass atomic elements in the alloy. However, most of the change in the thick shield *K* values was due to using OLTARIS calculations for equatorial Earth orbit ($K_{pure\ Al}$ = 1.005) instead of for 1 AU away from the Earth. Values of *K* derived from OLTARIS data were similar for solar minimum and maximum conditions, but slightly higher at solar maximum, reflecting the interplay of the shielding with the variation in spell out (GCR) spectral hardness at 1 AU during the solar cycle. Unfortunately, the OLTARIS calculations could not be made directly at orbit average vertical cutoff rigidities higher than 14 GV because of the limits of OLTARIS orbit definitions, so correction factors at higher cutoffs were extrapolated. In all cases, the dose rate corrections (relative to added atmosphere) were less than 1%.

The correction method was applied to CARI-7A calculations for the two levels of shielding at flight levels (FL) 300, 350, 400, 500, and 600 (30, 35, 40, 50 and 60 thousand feet) and a polar route flight (Figure 1) from New York to Beijing (KJFK to ZBBA), for near solar minimum (Jan. 1998) and solar maximum (Jan 2002).[6] The polar route cruised at FL 350, and is available at https://flightplandatabase.com/plan/505420.

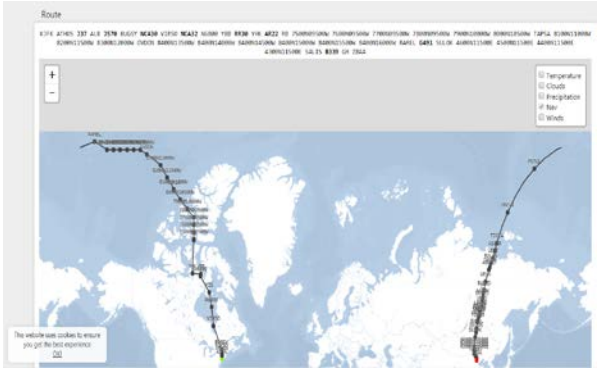

Figure 1. Transpolar route from New York City (KJFK) to Beijing (ZBBA).

There are a few caveats to using this method at all latitudes. Effective dose equivalent is the closest analog to effective dose OLTARIS can calculate. Also, the shielding effectiveness adjustments made for geomagnetic effects are based on orbit averaged effective vertical cutoff rigidities, while the atmospheric calculations with CARI-7A use the point values interpolated from tables.[7-12] A third consideration is that the version of HZETRN used for radiation transport in OLTARIS does not include secondary muon production (it is not important in the intended application of dosimetry in lightly shielded spacecraft), but instead creates additional neutrons.[13,14] In the atmosphere, this leads to effective dose rate estimates that are too high at great depths. How much error this could cause in this application, where ratios are used, is unknown. It was for this reason that we have limited the use of the OLTARIS results to near 50 g/cm^2 (a shield depth before muon buildup is very important, but after heavy ion primaries are mostly gone).

III. Results

Effective dose rates and shielding effectiveness data representative of a B-737 and B-747 are shown in figures 2-11. At typical modern passenger airline cruise altitudes (FL 300 to FL 400), the alloy shielding almost always reduces the dose rate by a few percent. A maximum dose reduction of 3% is seen at 0 GV vertical cutoff rigidity at FL 600. The benefit decreases as depth increases and as vertical cutoff rigidity increases, such that at FL 400 and above the added Al-2024 shielding increases rather than decreases the effective dose rate at the highest vertical cutoff rigidities. The maximum increase in dose rate, 0.4%, occurs at FL 500 at 17 GV.

Results for the transpolar route from KJFK to ZBBA are summarized in Table 2. Disregarding structure has only a minor influence on flight dose. Treating the alloy as greater depth in air overestimates the effectiveness of the structure as a shield. With the aluminum alloy taken into account, the flight dose for the transpacific polar route cruising at FL 350 is reduced by about 1%.

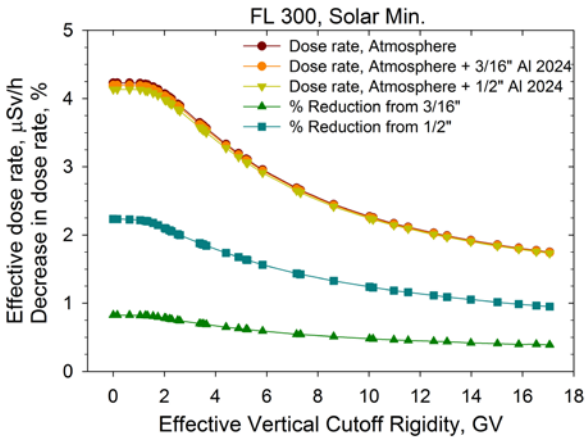

Figure 2. Relationships at FL 300 between effective vertical cutoff rigidity and effective dose rate and aircraft structure related percent reduction in effective dose rate for solar activity conditions near solar minimum (average for Jan. 1998). The alloy thicknesses of 3/16" (1.32 g/cm^2) and 1/2" (3.53 g/cm^2) are representative of a B-737 and B-747, respectively.

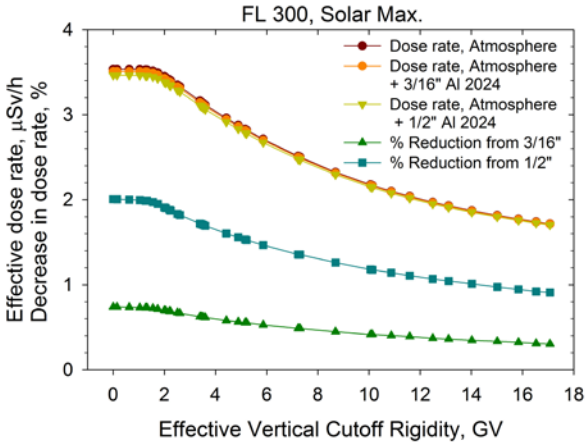

Figure 3. Relationships at FL 300 between effective vertical cutoff rigidity and effective dose rate and aircraft structure related percent reduction in effective dose rate for solar activity conditions near solar minimum (average for Jan. 2002). The alloy thicknesses of 3/16" (1.32 g/cm^2) and 1/2" (3.53 g/cm^2) are representative of a B-737 and B-747, respectively.

Table 2. Flight total effective doses for the KJFK-ZBBA route at the three levels of shielding studied.

Period	Effective dose (µSv)		
	Unshielded	1.32 g/cm^2 Alloy (Air*)	3.53 g/cm^2 Alloy (Air*)
Jan. 1998 (solar min.)	78.1	77.8 (77.6)	77.1 (76.6)
Jan. 2002 (solar max.)	61.0	60.7 (60.5)	60.3 (59.9)

* Substitution of shield mass with air instead of Al-2024.

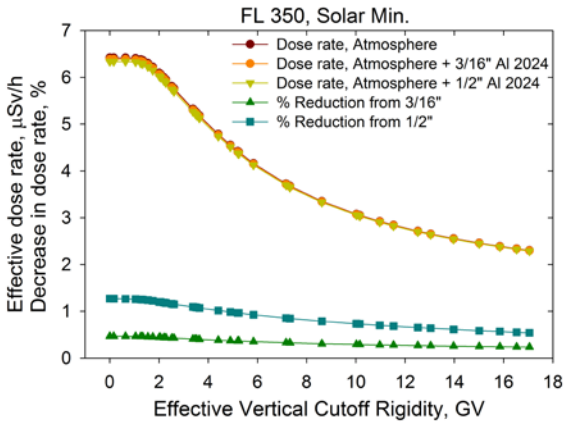

Figure 4. Relationships at FL 350 between effective vertical cutoff rigidity and effective dose rate and aircraft structure related percent reduction in effective dose rate for solar activity conditions near solar minimum (average for Jan. 1998). The alloy thicknesses of 3/16" (1.32 g/cm^2) and 1/2" (3.53 g/cm^2) are representative of a B-737 and B-747, respectively.

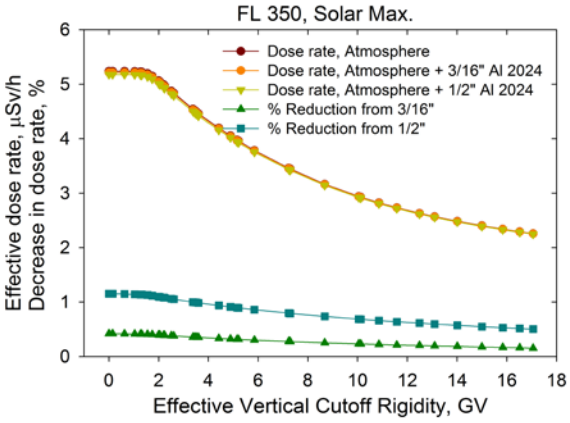

Figure 5. Relationships at FL 350 between effective vertical cutoff rigidity and effective dose rate and aircraft structure related percent reduction in effective dose rate for solar activity conditions near solar maximum (average for Jan. 2002). The alloy thicknesses of 3/16" (1.32 g/cm^2) and 1/2" (3.53 g/cm^2) are representative of a B-737 and B-747, respectively.

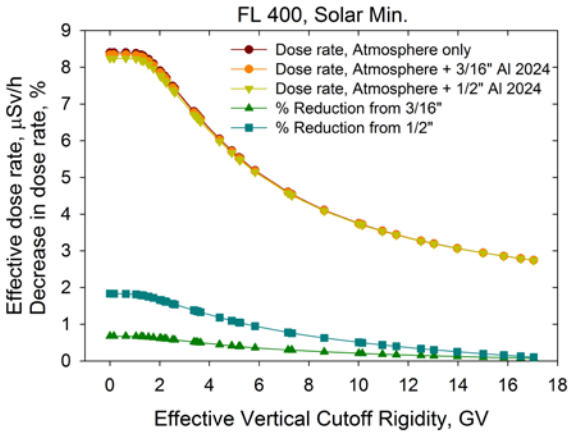

Figure 6. Relationships at FL 400 between effective vertical cutoff rigidity and effective dose rate and aircraft structure related percent reduction in effective dose rate for solar activity conditions near solar minimum (average for Jan. 1998). The alloy thicknesses of 3/16" (1.32 g/cm^2) and 1/2" (3.53 g/cm^2) are representative of a B-737 and B-747, respectively.

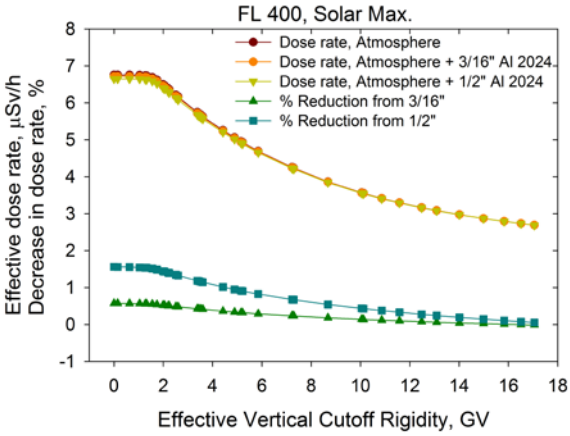

Figure 7. Relationships at FL 400 between effective vertical cutoff rigidity and effective dose rate and aircraft structure related percent reduction in effective dose rate for solar activity conditions near solar maximum (average for Jan. 2002). The alloy thicknesses of 3/16" (1.32 g/cm^2) and 1/2" (3.53 g/cm^2) are representative of a B-737 and B-747, respectively.

IV. Discussion

Results of this study are consistent with calculations by Battistoni, et al. of effective dose rates using FLUKA and an A-340 model at FL 350,[2,15] finding that including aircraft structure should reduce effective dose rates at 0.4

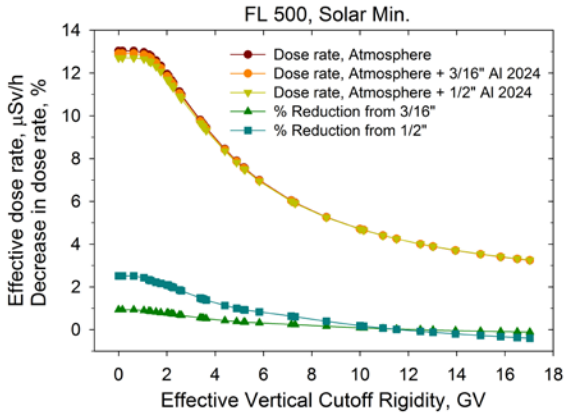

Figure 8. Relationships at FL 500 between effective vertical cutoff rigidity and effective dose rate and aircraft structure related percent reduction in effective dose rate for solar activity conditions near solar minimum (average for Jan. 1998). The alloy thicknesses of 3/16" (1.32 g/cm^2) and 1/2" (3.53 g/cm^2) are representative of a B-737 and B-747, respectively.

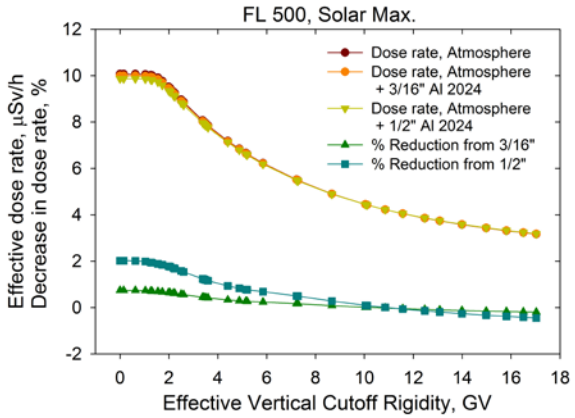

Figure 9. Relationships at FL 500 between effective vertical cutoff rigidity and effective dose rate and aircraft structure related percent reduction in effective dose rate for solar activity conditions near solar maximum (average for Jan. 2002). The alloy thicknesses of 3/16" (1.32 g/cm^2) and 1/2" (3.53 g/cm^2) are representative of a B-737 and B-747, respectively.

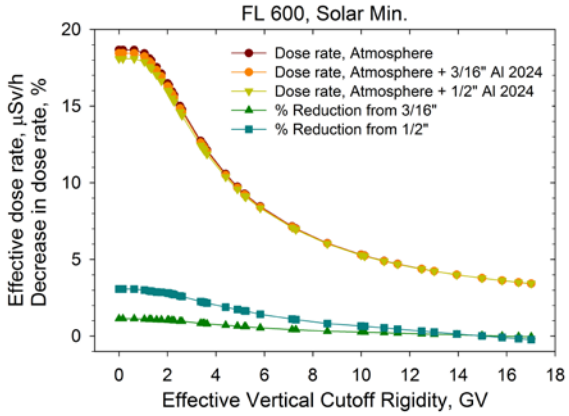

Figure 10. Relationships at FL 600 between effective vertical cutoff rigidity and effective dose rate and aircraft structure related percent reduction in effective dose rate for solar activity conditions near solar minimum (average for Jan. 1998). The alloy thicknesses of 3/16" (1.32 g/cm^2) and 1/2" (3.53 g/cm^2) are representative of a B-737 and B-747, respectively.

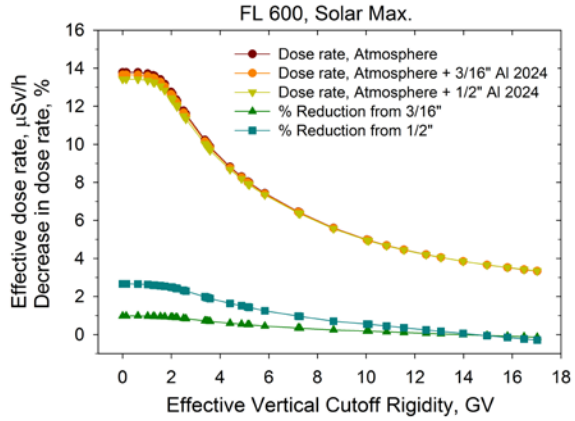

Figure 11. Relationships at FL 600 between effective vertical cutoff rigidity and effective dose rate and aircraft structure related percent reduction in effective dose rate for solar activity conditions near solar maximum (average for Jan. 2002). The alloy thicknesses of 3/16" (1.32 g/cm^2) and 1/2" (3.53 g/cm^2) are representative of a B-737 and B-747, respectively.

GV for crewmembers at commercial aircraft altitudes. They found the lowest reductions in effective dose rate in the cockpit (4-5%) and aisles (0-11%), where the flight and cabin crewmembers would be working, and a 7% average reduction once seated passenger locations were included (max. reduction of 14% for passengers in the center seating). These are greater reductions than our calculations indicate, but there are several differences: in addition to 5 mm of aluminum to represent the aircraft structure, they also included other contents of the aircraft when fully loaded such as fuel, passengers, and stowed luggage, which were not included in our models; their radiation model accounted more fully for anisotropy; and they based their calculation of effective dose on older recommendations

for tissue and radiation weighting factors.[16] While the interplay of secondary particle spectra, fluence to dose conversion and local shielding could lead to unexpected results, preliminary calculations using the method of the FAA report with polyethylene indicate that adding a few g/cm^2 of low atomic mass materials would further reduce effective dose rates relative to the unshielded case by a few percent, and bring our results into better numerical agreement.

Aside from the considerations discussed in the Methods, one must also consider that the FAA report shows the trend for aluminum to be increasingly like air as aircraft altitude decreases, suggesting the correction may be underestimating the effectiveness of the shielding. Also, shielding correction coefficients, *K*, are calculated from comparisons of effective dose equivalent, which is closely related to, but not the same as effective dose. Since dose equivalent is known to increase behind thin aluminum shields (relative to being unshielded), and organ dose equivalent is the basis for effective dose equivalent, the possibility that effective dose equivalent is not a good surrogate for effective dose in this application cannot be discounted. However, differences between the ICRP 2007 recommended effective dose and effective dose equivalent should be minimized when heavy ion contributions are minimal.[17]

V. Conclusion

These calculations indicate shielding is most effective on polar routes, where radiation is softest. Without accounting for aircraft loading, reductions in calculated effective dose rates by this method can be as large as a few percent. Accounting for structure may increase effective dose rates calculated for equatorial latitude routes, however, dose rates at equatorial latitudes are quite low when compared to those at polar latitudes, so this is not a serious health concern.

Acknowledgments

This work was funded by FAA Aeromedical Research task PSRLAB.AV9100.

References

1. Cox, J., "Ask the Captain: The challenges of transpolar flights," *USA Today*, 3:00 p.m. ET July 23, 2017 (Updated 8:15 a.m. ET July 24, 2017), available at https://www.usatoday.com/story/travel/columnist/cox/2017/07/23/transpolar-flights/499252001/ [cited 12 Dec. 2017].

2. Battistoni, G., Ferrari, A., Pelliccioni, M., Villari, R., "Evaluation of the dose to aircrew members taking into consideration the aircraft structures," *Advances Space Research*, Vol. 36, 2005, pp. 1645-1652.

3. Bottollier-Depois, J. F. et al., "Comparison of codes assessing radiation exposure of aircraft crew due to galactic cosmic radiation," European Radiation Dosimetry Group e.V, EURADOS Report 2012-03, Braunschweig, Germany, 2012.

4. Copeland, K., "Approximating Shielding Effects on Galactic Cosmic Radiation Effective Dose Rate Calculations during Extreme Altitude and Sub-Orbital Flights Using CARI-7/7A," FAA office of Aerospace Medicine technical report DOT-FAA-AM-17/8, Washington, DC, 2017.

5. Sandridge, C., "OLTARIS-An overview and recent updates," presented at the 2014 NASA Human Research Program Investigators Workshop, available at: www.hou.usra.edu/meetings/hrp2014/pdf/3056.pdf [cited 14, Jan 2016].

6. Copeland, K., "CARI-7A: Development and validation," *Radiation Protection Dosimetry*, 175(4), 2017, pp. 419-431.

7. O'Brien, K., "A 1×1 degree world grid of interpolated cosmic ray vertical cutoff rigidities from IGRF 1995, based on a 5×15 degree table calculated by D.F. Smart and M.A. Shea." Civil Aerospace Medical Institute, Oklahoma City, OK, 1999 (unpublished).

8. Shea, M. A., Smart, D. F. and McCall, J. R., "A five degree by fifteen degree world grid of trajectory determined vertical cutoff rigidities," *Canadian Journal of Physics*, Vol. 46, 1968, pp. S1028–S1101.

9. Shea, M. A. and Smart, D. F., "A world grid of calculated cosmic ray vertical cutoff rigidities for 1980.0,"*18th International Cosmic Ray Conference, Conference Papers*, Vol. 3, 1983, p. 415.

10. Smart, D. F. "Vertical geomagnetic cutoff rigidity latitude plots: IGRF 2000," Report for FAA CAMI contract AC-04-02566, Civil Aerospace Medical Institute, Oklahoma City, OK, 2005 (unpublished).

11. Smart, D. F. and Shea, M. A., "World grid of calculated cosmic ray vertical cutoff rigidities for epoch 1990," *25th International Cosmic Ray Conference, Conference Papers*, Vol 2, 1997, pp. 401-404.

12. Smart, D. F. and Shea, M. A., "World grid of calculated cosmic ray vertical cutoff rigidities from IGRF 2010, in partial fulfillment of FAA Procurement AAM-610-12-0157", Civil Aerospace Medical Institute, Oklahoma City, OK, 2012 (unpublished).

13. Wilson, J. W., et al., "Transport methods and interactions for space radiation," NASA RP-1257, 1991.

14. Wilson, J. W., et al. (1995) "HZETRN: Description of a free-space ion and nucleon transport and shielding computer program," NASA Technical Paper 3495, 1995.

15. Ferrari, A., Pelliccioni, M., and Villari, R., "Evaluation of the influence of aircraft shielding on the aircrew exposure through an aircraft mathematical model," Radiation Protection Dosimetry, Vol. 108, 2004, pp. 91-105.

16. International Commission on Radiological Protection (ICRP), "1990 Recommendations of the International Commission on Radiological Protection. London: Elsevier," ICRP Pub. 60, 1991.

17. International Commission on Radiological Protection (ICRP), "The 2007 Recommendations of the International Commission on Radiological Protection. London: Elsevier," ICRP Pub. 103, 2007.